



Society of Petroleum Engineers

SPE-190224-MS

An Experimental Study of Emulsion Flow in Alkaline Solvent Coinjection with Steam for Heavy-Oil/Bitumen Recovery

Kai Sheng, Francisco J. Argüelles-Vivas, Kwang Hoon Baek, and Ryosuke Okuno, The University of Texas At Austin

Copyright 2018, Society of Petroleum Engineers

This paper was prepared for presentation at the SPE Improved Oil Recovery Conference held in Tulsa, Oklahoma, USA, 14-18 April 2018.

This paper was selected for presentation by an SPE program committee following review of information contained in an abstract submitted by the author(s). Contents of the paper have not been reviewed by the Society of Petroleum Engineers and are subject to correction by the author(s). The material does not necessarily reflect any position of the Society of Petroleum Engineers, its officers, or members. Electronic reproduction, distribution, or storage of any part of this paper without the written consent of the Society of Petroleum Engineers is prohibited. Permission to reproduce in print is restricted to an abstract of not more than 300 words; illustrations may not be copied. The abstract must contain conspicuous acknowledgment of SPE copyright.

Abstract

Water is the dominant component in steam injection processes, such as steam-assisted gravity drainage (SAGD). The central hypothesis in this research is that in-situ oil transport can be enhanced by generating oil-in-water emulsion, where the water-continuous phase acts as an effective oil carrier. As part of the research project, this paper presents an experimental study of how oil-in-water emulsion can improve oil transport in porous media at elevated temperatures from 373 K to 443 K.

Diethyl amine (DEA) was selected as the organic alkali to form oil-in-water emulsions with Athabasca bitumen and NaCl brine at 1000 ppm salinity and 0.5 wt% alkali concentration. This composition had been confirmed to be optimal in terms of oil solubility in the water-external emulsion phase at a wide range of temperatures. Then, flow experiments with a glass-beads pack were conducted to measure effective viscosities for emulsion samples at shear rates from 5 to 29 sec^{-1} .

Results show that the oil-in-water emulsions were more than 18 times less viscous than the original bitumen at 373 and 403 K. At an estimated shear rate of 5 sec^{-1} , for example, the emulsion viscosity was 12 cp at 373 K, at which the bitumen viscosity was 273 cp. The efficiency of in-situ bitumen transport was evaluated by calculating bitumen molar flow rate under gravity drainage with the new experimental data. Results show that oil-in-water emulsion can enhance in-situ molar flow of bitumen by a factor of 64 at 403 K and 95 at 373 K, in comparison with the gravity drainage of oil-water two phases in conventional SAGD. This is mainly because the mobility of the bitumen-containing phase is enhanced by the reduced viscosity and increased effective permeability. A marked difference between alkaline solvents and conventional hydrocarbon solvents is that only a small amount of alkaline solvent enables to enhance in-situ transport of bitumen.

Introduction

Steam-assisted gravity drainage (SAGD) is the in-situ recovery technique widely used for bitumen production. SAGD requires two horizontal wells, several meters apart vertically: the upper well is for steam injection, and the lower well is for production. Wet steam of high quality is injected into the bitumen reservoir, and it condenses near thermal fronts. The latent heat of the injected water is the main source

of energy for reservoir heating. Although a small fraction of the heat is used for heating bitumen, SAGD effectively utilizes the sensitivity of bitumen viscosity to temperature along the edge of a high-temperature steam chamber.

SAGD needs a large amount of water and energy to generate steam, which makes it a major source of CO₂ emissions (Kim et al. 2017). Cumulative steam-to-oil ratio (CSOR), defined as volume ratio of injected water (cold-water equivalent) and produced oil, is an indicator of energy efficiency in steam-based recovery methods. Shen (2013) stated that CSOR has to be controlled below 4 m³/m³ for a SAGD process to be profitable. To improve the energy efficiency, coinjection of steam and different solvents have been studied in the literature, such as n-alkanes and condensates (Nasr et al. 2003; Gates 2007; Ivory et al. 2008; Li et al. 2011a and 2011b; Keshavarz et al. 2014 and 2015).

Investigations into solvent-SAGD phase behavior have shown that in general a better performance of these processes is expected as carbon number of the injected solvent increases. (Li et al. 2011a; Mohebbati et al. 2012; Keshavarz et al. 2015). Pilot tests, such as EnCana's SAP pilot and Imperial Oil's LASER, have demonstrated the potential of hydrocarbon solvent-SAGD to improve the bitumen recovery and reduce the CSOR (Nasr et al. 2003; Gates 2007; Gupta et al. 2005; Gupta and Gittins 2006; Leaute 2002; Leaute and Carey 2007; Li et al. 2011a b; Keshavarz et al. 2014 and 2015). However, the economic feasibility of solvent-SAGD can be highly uncertain because of the substantial costs associated with solvents and their treatment, and because the solvent recovery depends on reservoir heterogeneity.

Recently, Sheng et al. (2018) showed that water, the dominant component in a SAGD process, can be used as a solvent carrier to improve the efficiency of SAGD. They conducted a numerical simulation study of dimethyl ether (DME), a water soluble solvent. In their simulations, DME-SAGD was able to achieve 35% lower CSOR and 30% faster bitumen drainage at an early stage of coinjection than SAGD, and 15% more solvent recovery than n-butane-SAGD, as a result of DME's solubility in both water and bitumen. Other researchers have also studied phase behavior and thermophysical properties of mixtures of bitumen and DME (Baek et al. 2017; Haddadnia et al. 2018). In these studies, DME was used as a viscosity reducer for bitumen and heavy oil.

All methods mentioned above depend mainly on the viscosity reduction by temperature and/or dilution by condensed solvent near the edge of a steam chamber. However, it is also possible to enhance in-situ bitumen transport by making oil-in-water emulsions, where the water-external phase acts as an effective carrier of bitumen even at low temperatures. One way to make such emulsions is to activate acidic components in the in-situ bitumen as natural surfactants by adding organic alkali to steam. Baek et al. (2018) reported that Athabasca bitumen could be completely emulsified in water at low salinities (<1000 ppm) and low alkali concentrations in brine (<5 wt%) from 293 K to 373 K at atmospheric pressure. The low concentration of alkali required to emulsify bitumen is advantageous because the project's economics would be less affected by reservoir uncertainties.

The use of alkalis has been studied for heavy oil reservoirs in which steam injection is not an attractive option. Waterflooding processes such as alkaline flooding, alkaline-surfactant (AS), alkali-polymer (AP) and alkali-cosolvent-polymer (ACP) have the purpose of achieving ultra-low interfacial tension, emulsification and transport of heavy oil in water, and/or improvement of sweep efficiency through water-in-oil or oil-in-water emulsions (Liu et al. 2006 and 2007; Bryan and Kantzas 2007a b; Bryan et al. 2008; Dong et al. 2009; Kumar et al. 2012; Pei et al. 2013; Fortenberry et al. 2015; Xiao et al. 2017).

Some attempts have been also made to emulsify heavy oil and bitumen in water through steam-surfactant coinjection. Lu et al. (2017) and Zeidani and Gupta (2013) used commercially available surfactants with strong hydrophilicity to generate oil-in-water emulsions to improve bitumen recovery. Srivastava and Castro (2011) applied a class of surfactants called thin film spreading agents to enhance the cyclic steam stimulation method in Canadian heavy oil reservoirs.

Only two studies have focused on alkalis as additives to steam for SAGD. [Kim et al. \(2017\)](#) studied an alkaline-based SAGD process in a micro model to explain recovery mechanisms at the pore scale. They found that the emulsification of bitumen into water and the alteration of wettability towards a water-wet state were the mechanisms that enhanced bitumen recovery. More recently, [Baek et al. \(2018\)](#) demonstrated that a small amount of organic alkali, DEA, can form oil-in-water emulsions when mixed with brine and bitumen. Their phase behavior study showed that low alkali concentrations and salinity below 1,000 ppm are favorable conditions to form a single phase of bitumen-rich oil-in-water emulsion. [Baek et al. \(2018\)](#) also showed that, in comparison with bitumen, these emulsions were three to four orders of magnitude less viscous at 298 K and two orders of magnitude at 323 K.

However, no research has been conducted on the capability of oil-in-water emulsions as a bitumen carrier in porous media. Then, the objective of this research is to investigate the in-situ bitumen transport by oil-in-water emulsions created by adding DEA to Athabasca bitumen and 1000 ppm NaCl brine. The concentration of DEA in the brine was set to 0.5 wt% based on the phase behavior study of [Baek et al. \(2018\)](#). The main novelty of this research lies in the new experimental data for emulsion phase behavior and rheological properties at 35 bars and temperatures up to 443 K. The results are used to analyze the bitumen molar flow rates under gravity drainage for oil-in-water emulsions (DEA-SAGD) and two-phase flow of oil and water (conventional SAGD).

This paper is structured as follows. Section 2 introduces the experimental materials and methods of phase behavior tests, density measurements, and effective viscosities in a porous medium. Section 3 presents the experimental results and detailed analysis of them on the basis of a gravity drainage equation.

Experimental materials and methods

This section presents the materials, apparatus, and procedures used for the experimental part of this research.

Materials

A dehydrated Athabasca bitumen sample was used for this research, and analyzed by a commercial lab (Exova laboratory, Edmonton, Alberta, Canada). The molecular weight was measured to be 532 g/mol by the freezing point depression method. Compositional analysis showed 24.5 wt% saturates, 39.6 wt% aromatics, 19.6 wt% resin I, 1.6 wt% resin II, and 17.8 wt% asphaltenes. The density of the bitumen was 0.985 g/cm³ at 335 K and atmospheric pressure. The total acid number (TAN) of the bitumen sample was measured to be 3.56 mg-KOH/g-oil using the method of [Fan and Buckley \(2007\)](#). This acid number indicates that bitumen contains a good amount of acidic components, which can be activated as natural surfactants in a high pH aqueous solution.

In this research, oil-in-water emulsions were prepared by mixing the bitumen sample with an aqueous solution with 0.5wt% of diethylamine (DEA) and 1000 ppm of NaCl. The brine was made with de-ionized water. The DEA was provided by Sigma-Aldrich with a purity of 99.5%. The pH of the aqueous solution with 0.5% DEA and 1000 ppm of NaCl was measured to be 10.48.

Approximately 70 mL of a brine/DEA/bitumen mixture was prepared for the density and phase behavior measurements and the emulsion flow tests in a glass beads pack. An aqueous solution of 0.5 wt% DEA and 1000 ppm NaCl was prepared first. Then, this solution was mixed with the bitumen at the volume ratio of 7:3 at atmospheric pressure and 296 K. The mixture was sealed and heated to 353 K, and then it was stirred for one day. The mixture was left for additional two days in the accumulator before injected into the density meter or the glass beads pack, as will be shown in the following subsections.

Emulsion density and phase behavior measurements

[Baek et al. \(2018\)](#) studied phase behavior of the same mixture (30 vol% Athabasca bitumen + 70 vol% aqueous solution of 0.5 wt% DEA and 1,000 ppm NaCl) at atmospheric pressure and temperatures up to 373 K as part of their research. The pressure and temperature conditions in [Baek et al. \(2018\)](#) were limited

because glass pipettes were used for more general observation of phase behavior. In this research, phase behavior of this specific mixture was studied at 373 K, 403 K, and 443 K, at 35 bars, which are more relevant to SAGD operations.

Phase densities were measured by an in-line densitometer (Anton Paar) for this mixture. In-line density measurement also enables to detect any phase boundary, and phase amounts at these high-temperature-pressure conditions without direct visual observation. Measured data will be used to analyze the bitumen transport by oil-in-water emulsion in a later section.

Figure 1 shows the setup for density and phase behavior measurements for water/bitumen/DEA emulsions. The setup consists of two pumps, two accumulators, an in-line density meter, a pressure gauge, and an oven. One accumulator was used for the mixture to be injected, and the other for the effluent side of the density meter. An Omega pressure gauge (model PX459-2.5KGI-EH), located close to the inlet of the density meter, was used to measure the absolute pressure of the system.

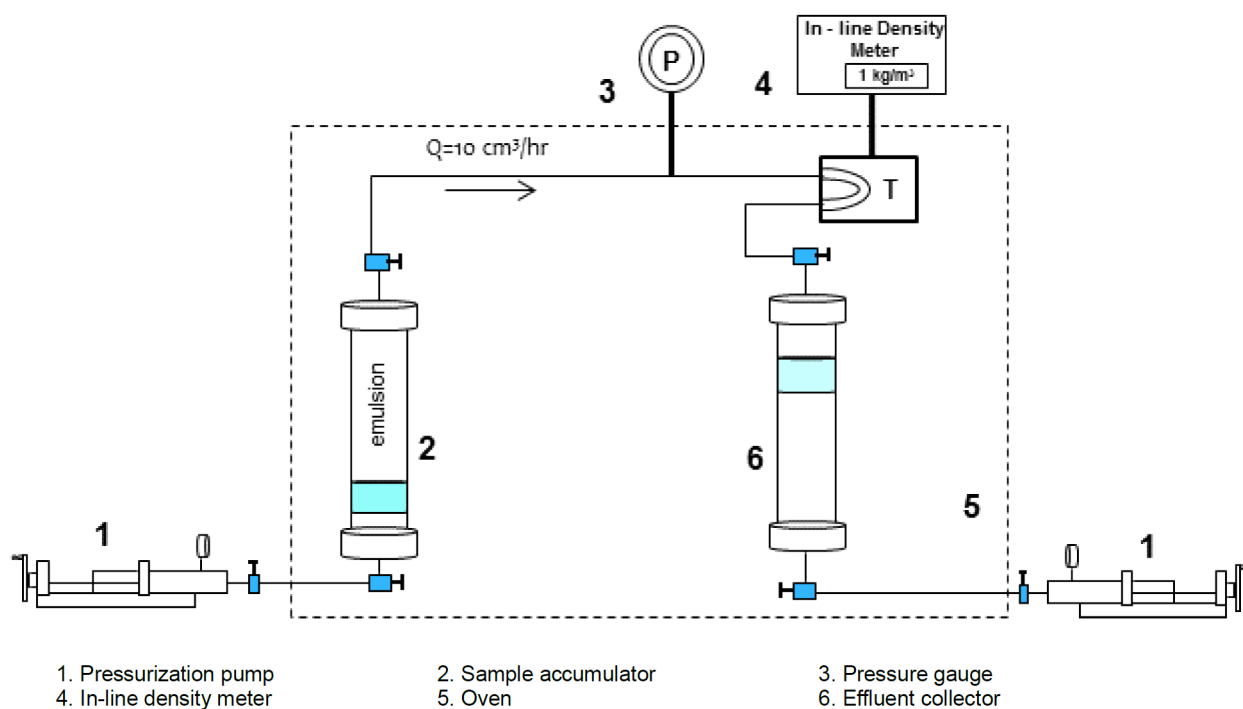


Figure 1—Schematic of the experimental set up for measuring density and for detecting phases for water/bitumen/DEA mixtures

The fluid sample passes through a measuring cell that accommodates a U-shaped tube where the fluid density is measured. This density meter is capable of measuring fluid densities from 0 to 3000 kg/m³ with an accuracy of $\pm 1 \text{ kg/m}^3$. The density meter was calibrated with water and nitrogen for pressures from 1.01 to 100 bars and temperatures in the range from 293 to 473K. A Despatch oven (LAC2-18-8) was used to heat up the system and to control the temperature. A monitor outside the oven is connected to the in-line density meter to display measured densities, pressures and temperatures. The accuracy levels of the temperature and pressure gauges are $\pm 0.1^\circ\text{C}$ and $\pm 0.08\%$ best straight line, respectively.

Prior to each measurement, the in-line density measurement system was cleaned meticulously with a 50-50 vol% methanol/toluene mixture, dried with nitrogen, and vacuumed for at least 2 hours. Then, the system was filled with helium at 35 bars using the effluent accumulator (number 6 in Figure 1).

The pressure of the system was maintained through the effluent accumulator with an Isco pump that operated at the constant pressure mode during all experiments. To ensure that there were no leakages in the setup, the pressure was monitored at least for 5 hours. Next, the accumulator containing 70 mL of a water/

bitumen/DEA emulsion (previously aged at 353 K for two days) was placed inside the oven, connected to the in-line system through its upper valve, and pressurized to 35 bars. Then, the oven was turned on to reach the test temperature (373, 403 or 443 K). Once the system temperature stabilized, the upper valve of the emulsion accumulator was open. Then, the Isco pump controlling the same accumulator was switched to the constant flow rate mode. The flow rate was set to 10 mL/hr, and the helium was displaced from the system and collected in the effluent accumulator.

The density of flowing fluid was recorded every second once the mixture reached the density meter. If there was a change in density, indicating a phase boundary, the sample was collected for compositional analysis. For such a case, a new accumulator for storing the effluent was connected to the system, and the experiment was re-started to measure the density of the remaining sample.

Flow of oil-in-water emulsion through a porous medium

Effective viscosities were measured for oil-in-water emulsions at different shear rates through a glass beads pack. Measurement of the effective viscosity of emulsions is based on [Sadowski and Bird \(1965\)](#), who used a generalized Darcy's law for Newtonian and non-Newtonian fluids. Brine is a Newtonian fluid, and oil-in-water emulsion is generally a non-Newtonian fluid. Assuming the same interstitial structures, permeability, porosity, cross sectional area and length, the effective viscosity of emulsion can be determined by

$$\mu_{\text{emulsion}} = \frac{\Delta P_{\text{emulsion}}}{\Delta P_{\text{brine}}} \mu_{\text{brine}}, \quad (1)$$

where μ is viscosity, and ΔP is the pressure drop. Note that the emulsion viscosities so determined are "effective" values under the measured $\Delta P_{\text{emulsion}}$ because all other parameters are assumed unchanged in comparison to brine flow.

[Figure 2](#) shows the setup for the coreflooding tests. This coreflooding setup consists of two pumps, four accumulators, a glass beads pack, a pressure transducer, an absolute pressure gauge and a temperature gauge. A glass-beads pack was placed horizontally inside the oven. The glass-beads holder is a 1/4" stainless tube with a length of 0.5 m. The capacity of the tube is 8.2 mL. The pressure drop along the porous medium was recorded by an Emerson differential pressure transducer. The pressure transducer is capable of measuring pressure drops from 0 to 2.1 bars with an accuracy of 0.001 bars. A thermometer (RTD model PR-11-2-100-1/8-12-E) was placed near the inlet of the glass beads pack to monitor the temperature of the oil-in-water emulsions.

The porous medium inside the pipe is a reproduction of a fine-grained oil sand sample from the Middle McMurry Formation ([Mahammadmoradi et al. 2017](#)), which is a major bitumen production zone in Athabasca, Alberta, Canada. The porous medium made is a glass-bead pack with particle diameters ranging from 63 to 500 μm with a median diameter of 169 μm . The two ends were covered by stainless screens with an opening size of 53 μm to prevent beads production and the crumbling of the pack during the emulsion flow tests. The porosity and absolute permeability of the sand pack were measured with brine at 373 and 403 K and 35 bars several times. The resulting porosity and permeability were on average 35% and 11.6 Darcy, respectively, and were not sensitive to temperature.

Two accumulators (A and B in [Figure 2](#)) containing the brine and water/bitumen/DEA emulsion, respectively, were placed inside the oven, connected to the experimental setup, and pressurized to 35 bars. Two more accumulators (C and D in [Figure 2](#)) for 50 mL of distilled water were connected on the downstream side of the outlet valve of the glass beads holder to store the effluent, and hold the pressure of the experiments. Accumulators C and D operated at a constant backward flow rate during the flow tests. The oven was heating to the temperature of the test, and the setup was vacuumed for at least 4 hours, including the tubings and the glass-beads pack. Once the test temperature became stable, the upper valve of the brine accumulator was opened to saturate the system with brine. The porosity of the packing was calculated. Then, the pump that controlled the brine accumulator was switched to the constant flow rate mode. After that, the

outlet valve of the glass-beads pack and the valve of accumulator C were opened. The pressure drop along the beads pack was recorded, and the brine was collected in accumulator C.

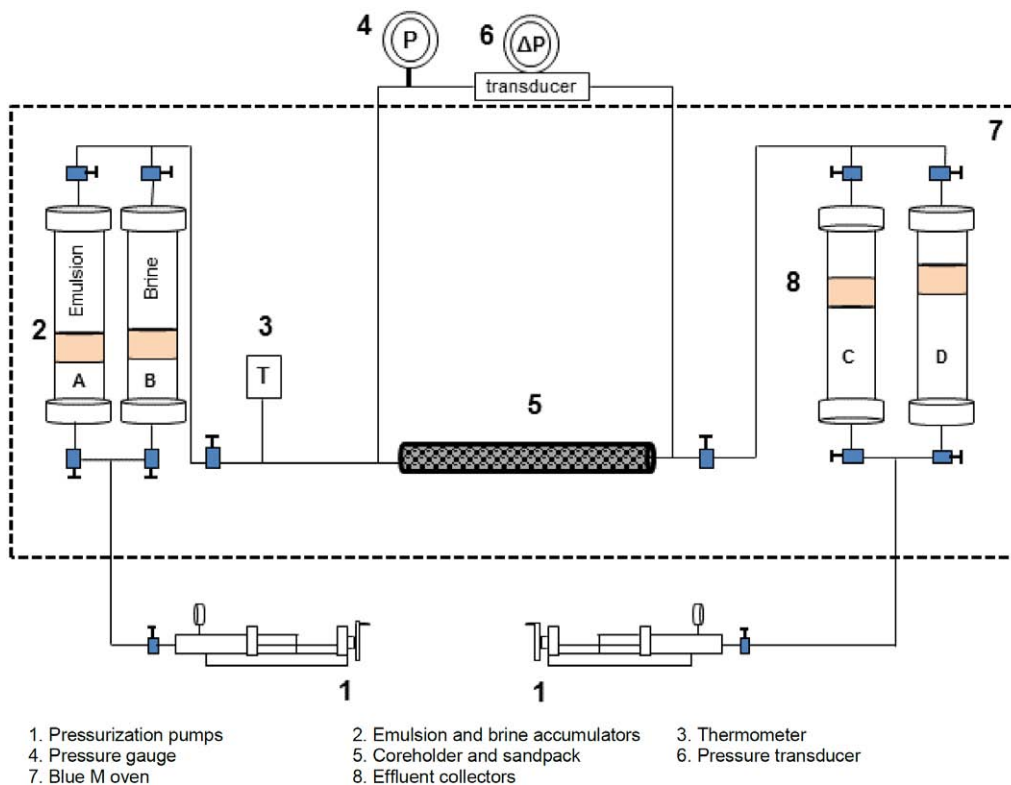


Figure 2—Schematic of the experimental set up for measuring effective viscosities of oil-in-water emulsion with a glass bead pack.

The brine accumulator was isolated after measuring the porosity and absolute permeability. The pump controlling the emulsion accumulator was switched to a constant flow rate to displace the brine and saturate the glass beads pack with the water/bitumen/DEA emulsion. Once the glass beads pack was saturated by the emulsion, the pressure drop was measured to obtain an effective viscosity of emulsion. Accumulator D was used to store the water/bitumen/DEA emulsion on the effluent side.

Before starting a new experiment, the system was cleaned thoroughly with a 50-50 vol% methanol/toluene mixture until the initial porosity and absolute permeability were restored. Then, the system was dried under vacuum. The effective viscosities of emulsions were obtained at 373 and 403 K at 35 bars and different shear rates.

Results and discussion

Density measurement and phase behavior

Figure 3 shows the measured densities at 35 bars and 373 K, 403 K, and 443 K. The horizontal axis is dimensionless cumulative volume, defined as the cumulative injected volume divided by the total volume of the water/bitumen/DEA mixture. This axis can represent phase saturations. Table 1 shows the measured emulsion densities along with the densities of water and bitumen taken from National Institute of Standards and Technology (NIST) and Baek et al. (2018). The bitumen used by Baek et al. (2018) and in this research is denser than water by 2.6, 7.6 and 20.4 kg/m³ at 373, 403 and 443 K, respectively.

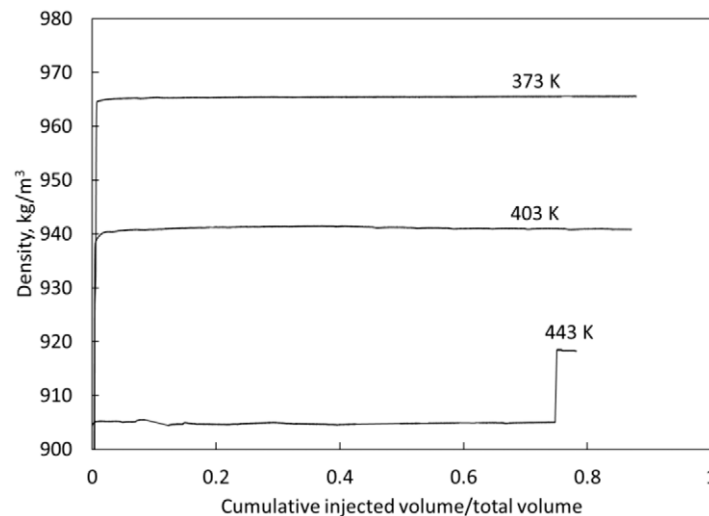


Figure 3—Densities measured are presented with respect to dimensionless cumulative injected volume at 35 bars and 373, 403 and 443 K. The dimensionless cumulative injected volume is defined as cumulative injected volume divided by total volume. There is only a single-phase emulsion at 373 K and 403 K.

Table 1—Water, bitumen and measured emulsion densities (kg/m³) at 35 bars and 373 K, 403 K, and 443 K.

	373 K	403 K	443 K
Water (NIST)	959.9	936.8	899.4
Bitumen (Baek et al. 2017)	962.3	944.2	919.7
Measured emulsion density in this research	965.5	941.1	904.8

Figure 3 presents that the mixture formed a single-phase emulsion at 373 and 403 K at 35 bars. All the bitumen was emulsified within the water-continuous phase. Single-phase water-external emulsions for the same mixture were also observed at atmospheric pressure at temperatures up to 373 K in Baek et al. (2018). At 373 K, the emulsion was calculated to be approximately 2 kg/m³ denser than the bitumen by using the density model of the Athabasca bitumen sample (Baek et al. 2017). Although the bitumen samples used in this research and in Baek et al. (2017) were taken from the same 5-gallon container, this unexpected result may be attributed to some non-homogeneity of bitumen composition inside the container at room temperature. At 403 K, the emulsion density was between water and bitumen densities. A single-phase oil-in-water emulsion is expected to contribute to enhancing in-situ bitumen transport by increasing effective permeability to the highly-mobile water phase that contains bitumen.

Two phases were detected at 443 K. The first phase represented 75 vol%, which was observed to be an oil-in-water emulsion at room temperature and atmospheric pressure. The second phase was a bitumen-rich phase (918.0 kg/m³) as indicated by the densities of bitumen (919.7 kg/m³) at 443 K and 35 bars. Visual inspection at room temperature indicated that the second phase was a bitumen-rich phase with dissolved or dispersed water. Composition analysis showed that the first phase contained about 12 vol% (0.46 mol%) of bitumen and the second phase about 85 vol% (16.2 mol%) of bitumen. These results indicate that the oil-in-water emulsion may become less stable at higher temperature, but the presence of natural surfactants still makes some change in oil and water saturations.

Effective viscosity of emulsion in an oil-sand type porous medium

Figure 4 and Table 2 show the effective viscosity data for the emulsion at 373 and 403 K at 35 bars. Emulsification of bitumen into water by natural surfactants can be an effective way to transport bitumen if bitumen is much more viscous than water; e.g., at 403 K or lower temperatures.

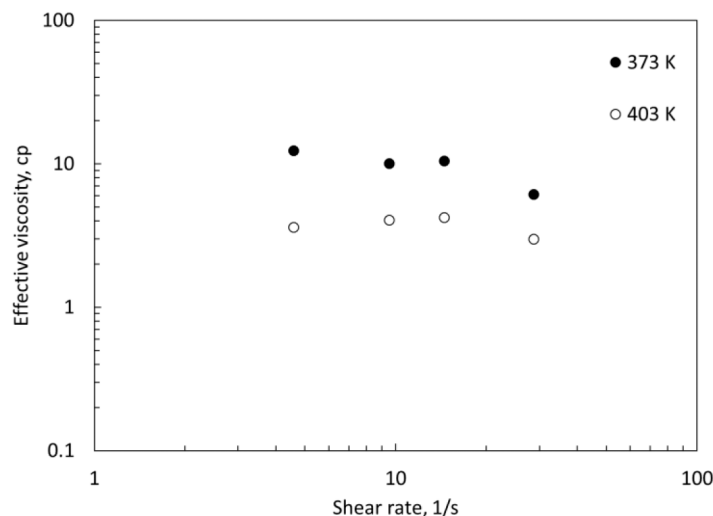


Figure 4—Calculated effective viscosities of oil-in-water emulsions at different shear rates at 35 bars and 373 and 403 K. The viscosity of the 1000 ppm brine is assumed to be the same as pure water viscosity; 0.28 and 0.21 cp at 373 and 403 K, respectively.

Table 2—Calculated effective viscosity (cp) for emulsions at 373 K and 403 K and 35 bars, at shear rates from 5 to 29 s⁻¹.

Temperature, K	5 s ⁻¹	10 s ⁻¹	15 s ⁻¹	29 s ⁻¹
373	12.40	10.08	10.51	6.10
403	3.63	4.07	4.23	3.00

At 373 K, the emulsion showed weakly shear-thinning behavior at shear rates from 5 to 29 s⁻¹. Data from 10 to 15 s⁻¹ show that the effective viscosity slightly increased with increasing shear rate. The emulsion viscosity at 403 K is 2 to 3 times lower than that at 373 K. At 403 K, the emulsion viscosity did not show a clear sensitivity to shear rate from 5 to 29 s⁻¹. The effective viscosity of emulsion is 22 times lower than the bitumen viscosity at 373 K and 18 times at 403 K. An average effective viscosity is taken from the data between 5 and 10 sec⁻¹ at each temperature to calculate molar flow rates of bitumen in the next section.

Analysis of bitumen flow rate in SAGD

Experimental data presented in this paper and Baek et al. (2018) show that it is possible to form single-phase oil-in-water emulsions by adding DEA to mixtures of bitumen and brine. This subsection is concerned with a question as to how the bitumen transport by oil-in-water emulsion is compared with that by two-phase flow of oil and water in conventional SAGD. This question is addressed by calculating molar flow rates of Athabasca bitumen under gravity drainage for assumed in-situ conditions beyond the edge of a steam chamber as follows:

- The pressure is 35 bars.
- The water-to-oil ratio is 7:3, which corresponds to the overall volumetric composition of produced fluid in SAGD at a steam-to-oil of 2.3.
- NaCl brine salinity is 1,000 ppm, which is higher than usual salinity levels of produced water in SAGD
- The DEA concentration in the aqueous solution is 0.5 wt%.

Darcy's law applied to the edge of a steam chamber at elevation z gives

$$U_o(z) = -k\rho_o g \sin \theta / \mu_o = -kg \sin \theta / v_o, \quad (2)$$

where U_o is the Darcy flow velocity for the oil-rich phase along the chamber edge, k is absolute permeability, and θ is the angle of the flow at elevation z . The symbols ρ_o , μ_o , and ν_o are mass density, viscosity, and kinematic viscosity of the oil-rich phase, respectively. Integrating U_o for a cross section perpendicular to the edge of a steam chamber, flow rate of the oil-rich phase at elevation z is

$$q_o(z) = \int_0^{\xi_L} U_o \Delta y d\xi = - \int_0^{\xi_L} (kg \sin \theta / \nu_o) \Delta y d\xi = -kg \sin \theta \Delta y I_o, \quad (3)$$

where k is assumed to be constant with ξ . The ξ direction is perpendicular to the steam chamber edge. $\xi = 0$ at the edge of a steam chamber. ξ_L is the distance from the steam-chamber edge where oil-rich-phase flow diminishes. Δy is the unit length along the horizontal section of a SAGD well pair. " I_o " is defined as

$$I_o(z) = \int_0^{\xi_L} \frac{1}{\nu_o} d\xi. \quad (4)$$

Molar flow rate of the bitumen component in the oil-rich phase is then calculated as

$$q_{bo}(z) = -kg \sin \theta \Delta y I_{bo}, \quad (5)$$

$$\text{where } I_{bo}(z) = \int_0^{\xi_L} \left(k_{ro} \underline{\rho}_o x_{bo} / \nu_o \right) d\xi. \quad (6)$$

In [equation 6](#), k_{ro} is relative permeability of the oil-rich phase, $\underline{\rho}_o$ is the molar density of the oil-rich phase, and x_{bo} is the concentration of the bitumen component in the oil-rich phase.

[Equation 3](#) was combined with local and global material balance equations along with a 1-D heat conduction model and a linear chamber edge in [Shi and Okuno \(2018\)](#). However, to do so for emulsified bitumen requires more comprehensive data for emulsion phase behavior at a wide range of temperatures at a specified pressure, which are quite expensive and beyond the scope of the current paper. With the data obtained in this research, therefore, a comparison is made between bitumen molar flow by oil-in-water emulsion and that in two-phase flow of oil and water in conventional SAGD in terms of the integrand of [equation 6](#). This comparison is based on the phase behavior data for the integrand at a given temperature at 35 bars. Note that the integrand takes into account the effective permeability of the phase that transports bitumen.

Mass densities and effective viscosities of the oil-in-water emulsion using DEA were obtained at 373 and 403 K and 35 bars. An average viscosity was taken between data at 5 and 10 sec^{-1} to represent the emulsion viscosity at each temperature. Molar density of the emulsion can be calculated as the measured mass density divided by the molecular weight of the mixture.

For the SAGD counterpart, ideal mixing was assumed for the calculation of densities for brine/bitumen mixtures. Viscosities of bitumen at 373, 403 and 443 K and 35 bars are 273, 66 and 19 cp, and those for water are 0.28, 0.21 and 0.16 cp. Viscosity of a water-containing oil phase was based on the SAGD liquid-viscosity model of [Venkatramani and Okuno \(2015\)](#). All the properties of water are from NIST's thermophysical property database, and properties of bitumen are from [Baek et al. \(2017\)](#).

The molar compositions, phase identity and phase saturations used for the molar flow rate calculation are tabulated in [Table 3](#). Phase equilibrium calculations were performed at 35 bars and from 373 and 443 K to determine the oil phase composition for the brine/bitumen mixture according to the Peng-Robinson EOS models by [Venkatramani and Okuno \(2014\)](#). To compare DEA-SAGD with SAGD, the same water-to-oil ratio (7:3) is assumed. At 443 K, the brine/bitumen/DEA mixture is approximated to have the same phase saturation and composition as the brine/bitumen mixture does, since the amount of bitumen in the emulsion was measured to be lower than 0.1 mol%. Corey's relative permeability models were assumed in the calculation:

$$k_{rw} = k_{rw}^o \left(\frac{S_w - S_{wr}}{1 - S_{wr} - S_{or}} \right)^n \quad (7)$$

$$k_{ro} = k_{ro}^o \left(\frac{1-S_w-S_{or}}{1-S_{wr}-S_{or}} \right)^m \quad (8)$$

Table 3—Molar composition, phase identity and phase saturation of the bitumen-rich phase in SAGD and DEA-SAGD in molar flow rate calculation. Compositions for oil phase in SAGD are obtained by phase equilibrium calculation with Venkatramani and Okuno's (2015) PR-EOS models. WOR in SAGD is assumed to be 7:3. At 443 K, amount of bitumen in the emulsion phase is neglected as the effective viscosity of the emulsion phase was not measured.

Temperature, K	Recovery process	Water mol%	Bitumen mol%	Solvent mol%	Bitumen-rich phase identity	Bitumen-rich phase saturation
373	SAGD	3.6	96.4	–	Oil Phase	0.30
	DEA-SAGD	98.4	1.5	0.1	Emulsion phase	1.00
403	SAGD	6.8	93.2	–	Oil phase	0.30
	DEA-SAGD	98.4	1.5	0.1	Emulsion phase	1.00
443	SAGD	13.6	86.4	–	Oil phase	0.30
	DEA-SAGD	13.6	86.4	0	Oil phase	0.30

where k_{rw} and k_{ro} are relative permeabilities for water and oil phases. k_{rw}^o and k_{ro}^o are endpoint relative permeabilities at irreducible oil saturation and connate water saturation, respectively. S_w , S_{wr} and S_{or} are water saturation, residual water saturation, and residual oil saturation, respectively. Exponents m and n determine the curvature of the relative permeabilities. Parameters for Corey's model for water-wet oil sands were taken from Keshavarz et al. (2014) as tabulated in Table 4.

Table 4—Parameters for Corey's relative permeability model as defined in equations 7 and 8.

Parameters	Values
S_{wr}	0.25
S_{or}	0.13
k_{rw}^o	0.30
k_{ro}^o	1.00
m	2
n	2

Figure 5 shows the evaluation of the integrand in equation 6 for the SAGD case from 373 to 515 K and DEA-SAGD case from 373 to 443 K at 35 bars. The integrand for the DEA-SAGD case is 95 times greater at 373 K and 64 times greater at 403 K, in comparison with that for the SAGD case. The integrand of the DEA-SAGD case at 373 K and 403 K cannot be reached by SAGD case even at the highest temperature, 515 K. Although this is taken as a preliminary evaluation of enhancement of in-situ bitumen transport, DEA-SAGD might offer substantial energy savings by enabling low-temperature operation. Since the emulsion droplets likely coalesce at higher temperatures, bitumen flow rate of DEA-SAGD may become similar to that of SAGD at 443 K. There may be an upper temperature limit (greater than 443 K in this particular composition) for the emulsification of bitumen in water by using DEA alone.

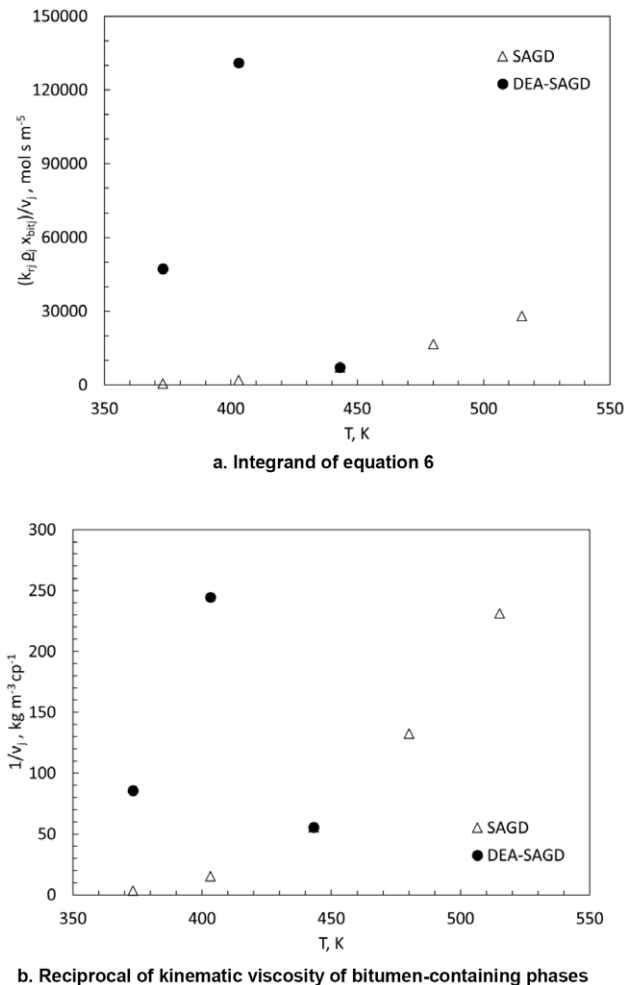


Figure 5—Bitumen molar flow rate analysis with the integrand of equation 6, and kinematic viscosity of bitumen-containing phases at 35 bars and temperatures from 373 to 443 K for DEA-SAGD and up to 515 K for SAGD. An average is taken between emulsion viscosities at 5 and 10 sec⁻¹ for the viscosity used for bitumen molar flow rate calculation.

Influential factors in the integrand were analyzed to understand potential mechanisms for DEA-SAGD. One of the factors is the reduction of the bitumen-rich phase viscosity by adding only 0.12 mol% of DEA. As shown in Figure 5b, the reciprocals of kinematic viscosity for the emulsion are 24 and 16 times greater than oil phase viscosity in SAGD at 373 and 403 K, respectively. This indicates that in terms of kinematic viscosity reduction, emulsion kinematic viscosities at 373 and 403 K are equivalent to the oil phase in the SAGD case at 465 and almost 515 K, respectively.

Also, the effective permeability of the bitumen-rich phase for DEA-SAGD (i.e. the emulsion phase) is calculated to be 13 times greater than that of the bitumen-rich phase of SAGD (i.e., the oil phase) at 373 K and 403K. In DEA-SAGD, the water-external phase can flow with a good amount of bitumen contained. In SAGD, however, bitumen flows as part of the oil phase with dissolved and/or dispersed water with a relative permeability of 0.075 in the current example. Even if oil-in-water emulsion is present with an excess oil phase (e.g., at different DEA concentrations), natural surfactants likely decrease the interfacial tension between the water and bitumen phases, which would improve the fluid mobilities.

Conclusions

DEA was studied as a potential additive to steam for improved SAGD. The main objective of this paper was to present a new set of experimental data for emulsion phase behavior and emulsion flow in a porous medium at elevated temperatures and pressures.

The oil-in-water emulsions studied were made by a mixture of an aqueous solution with 1000 ppm NaCl and 0.5 wt% DEA and Athabasca bitumen at a volume ratio of 7:3. Then, phase behavior and effective viscosities of the emulsions were measured with an in-line density meter and glass-beads-pack flow system at 35 bars and temperatures from 373 K to 443 K. Bitumen molar flow rate in DEA-SAGD was compared with that in SAGD with Darcy's law for gravity drainage using the experimental data. Conclusions are as follows:

- At 35 bars and from 373 K to 403 K, bitumen was totally emulsified into water by activating acidic components of the bitumen as natural surfactants. At 443 K, bitumen was only partly emulsified into water.
- The emulsion showed weakly shear-thinning behavior at 373 K and 35 bars. At 403 K, the emulsion viscosity did not show a clear sensitivity to shear rate from 5 to 29 s⁻¹.
- In-situ bitumen transport can be enhanced by emulsification of bitumen into water using DEA. The integrand in [equation 6](#) is an indicator of the bitumen flow capability in gravity drainage. The integrand for emulsified bitumen was calculated to be 95 to 64 times greater than that for SAGD with the overall DEA concentration of 0.12 mol% at 373 and 403 K. Bitumen transport for the DEA-SAGD case at 373 and 403 K was calculated to be even more efficient than that for SAGD at 515 K. There seems to be an upper temperature limit (greater than 443 K), above which using DEA alone may not be effective for emulsification of bitumen.
- The enhanced mobility of bitumen by emulsification comes from the reduced kinematic viscosity and the increased effective permeability of the emulsion phase that transports the bitumen component. In-situ transport of bitumen as oil-in-water emulsion can be more efficient than the bitumen transport as two-phase flow of oil and water in conventional SAGD, especially at relative low temperatures (e.g., below 403 K). Although not shown in this paper, sensitivity analysis showed that these conclusions are unlikely affected by the relative permeability model employed in the analytical calculations.

Acknowledgements

We gratefully acknowledge the financial support from Japan Canada Oil Sands Ltd. and the Chemical EOR Industrial Affiliates Project at the University of Texas at Austin. Ryosuke Okuno holds the Pioneer Corporation Faculty Fellowship in Petroleum Engineering at The University of Texas at Austin. The authors thank Dr. Gary A. Pope for sharing his equipment, and also Mr. Glen S. Baum for his assistance for this research.

Nomenclature

Roman Symbols

- g = gravitational constant, 9.8 m/s²
- I = parameter defined in [equation 4](#)
- k = absolute permeability, Darcy
- k_r = relative permeability
- m, n = parameters for Corey's relative permeability models
- P = pressure, bar
- q = molar flow rate, mol/s
- S = saturation
- U = Darcy's flow velocity
- x = mole fraction
- y = length of reservoir parallel to well pair, m

z = elevation from the production well on the chamber edge, m

Greek Symbols

α = reservoir diffusivity, m²/s
 θ = angle between tangent to chamber edge and horizontal line
 μ = dynamic viscosity, cp
 ν = kinematic viscosity, cp·m³/kg
 ξ = distance from perpendicular to chamber edge, m
 ρ = molar density, mole/m³
 ρ = mass density, mole/m³

Superscripts

o = endpoint

Subscripts

b = bitumen
 L = mobilized bitumen
 o = oil-rich phase
 or = residual oil
 w = water
 wr = residual water

Abbreviations

CSOR = cumulative steam-to-oil ratio
 DEA = diethyl amine
 DME = dimethyl ether
 EOS = equation of state
 ES-SAGD = expanding-solvent-SAGD
 MW = molecular weight, g/mol
 SAGD = steam-assisted gravity drainage
 SARA = saturates, asphaltenes, resins and aromatics
 SOR = steam-oil ratio
 WOR = water-to-oil ratio

References

- Baek, K., Sheng, K., Argüelles-Vivas, F.J., and Okuno, R. 2017. Comparative Study of Oil Dilution Capability of Dimethyl Ether and Hexane as Steam Additives for SAGD, SPE Annual Technical Conference and Exhibition, 9-11 October, San Antonio, Texas, USA. <https://doi.org/10.2118/187182-MS>
- Baek, K., Argüelles-Vivas, F.J., Okuno, R., Sheng, K., Sharma, H. and Weerasooriya, U.P. 2018. Organic Alkali as a Steam Additive for Improved SAGD: Experimental Study of Emulsion Phase Behavior and Viscosity, Canada Heavy Oil Technical Conference, 13-14 March, Calgary, Alberta, Canada. <https://doi.org/10.2118/189768-MS>
- Bryan, J. and Kantzas, A. 2007a. Potential For Alkali-Surfactant Flooding In Heavy Oil Reservoirs Through Oil-in-Water Emulsification. Canadian International Petroleum Conference, 12-14 June, Calgary, Alberta. <https://doi.org/10.2118/09-02-37>
- Bryan, J. and Kantzas, A. 2007b. Enhanced Heavy-Oil Recovery by Alkali-Surfactant Flooding. SPE Annual Technical Conference and Exhibition, 11-14 November, Anaheim, California, U.S.A. <https://doi.org/10.2118/110738-MS>
- Bryan, J., Mai, A. and Kantzas, A. 2008. Investigation Into the Processes Responsible for Heavy Oil Recovery by Alkali-Surfactant Flooding. SPE Symposium on Improved Oil Recovery, 20-23 April, Tulsa, Oklahoma, USA. <https://doi.org/10.2118/113993-MS>

- Cobos, S., Carvalho, M. S., & Alvarado, V. 2009. Flow of oil–water emulsions through a constricted capillary. *International Journal of Multiphase Flow* **35**(6): 507–515. <https://doi.org/10.1016/j.ijmultiphaseflow.2009.02.018>
- Dong, M., Ma, S. and Liu, Q. 2009. Enhanced heavy oil recovery through interfacial instability: A study of chemical flooding for Brintnell heavy oil. *Fuel* **88**: 1049–1056. <https://doi.org/10.1016/j.fuel.2008.11.014>
- Fan, T. and Buckley, J. 2007. Acid Number Measurements Revisited. *SPE Journal* **12**(04): 496–500. <https://doi.org/10.2118/99884-PA>
- Fortenberry, R., Kim, D., Nizamidin, N., Adkins, S., Arachchilage, G., Koh, H., Weerasooriya, U. and Pope, G. 2015. Use of Cosolvents To Improve Alkaline/Polymer Flooding. *SPE Journal* **20**(2). SPE-166478-PA. <https://doi.org/10.2118/166478-PA>
- Gates, I. D., 2007. Oil Phase Viscosity Behavior in Expanding-Solvent Steam-Assisted Gravity Drainage. *Journal of Petroleum Science and Engineering* **59** (1-2): 123–134. <https://doi.org/10.1016/j.petrol.2007.03.006>
- Gupta, S. C. and Gittins, S. D. 2006. Christina Lake Solvent Aided Process Pilot. *Journal of Canadian Petroleum Technology* **45** (9): 15–18. <https://doi.org/10.2118/2005-190>
- Gupta, S., Gittins, S. and Picherack, P. 2005. Field Implementation of Solvent Aided Process. *Journal of Canadian Petroleum Technology* **44** (11): 8–13. <https://doi.org/10.2118/05-11-TN1>
- Haddadnia, A., Azinfar, B., Zirrahi, M., Hassanzadeh, H. and Abedi, J. 2018. Thermophysical properties of dimethyl ether/Athabasca bitumen system. *The Canadian Journal of Chemical Engineering* **96**: 597–604. <https://doi.org/10.1002/cjce.23009>
- Ivory, J. J., Zheng, R., Nasr, T. N., Deng, X., Beaulieu, G., Heck, G. 2008. Investigation of Low Pressure ES-SAGD. Presented at 2008 SPE International Thermal Operations and Heavy Oil Symposium, Calgary, Alberta, Canada, October 20-23. <https://doi.org/10.2118/117759-MS>
- Keshavarz, M., Okuno, R., and Babadagli, T. 2014. Efficient Oil Displacement Near the Chamber Edge in ES-SAGD. *Journal of Petroleum Science and Engineering* **118**: 99–113. <https://doi.org/10.1016/j.petrol.2014.04.007>
- Keshavarz, M., Okuno, R., and Babadagli, T. 2015. Optimal Application Conditions for Steam/Solvent Coinjection. *SPE Reservoir Evaluation & Engineering* **18** (1):20–38. <https://doi.org/10.2118/165471-PA>
- Kim, M., Abedin, A., Lele, P., Guerrero, A. and Sinton, D. 2017. Microfluidic pore-scale comparison of alcohol- and alkaline-based SAGD processes. *Journal of Petroleum Science and Engineering* **154**: 139–149. <https://doi.org/10.1016/j.petrol.2017.04.025>
- Kokal, S. 2005. Crude-Oil Emulsions: A State-Of-The-Art Review. *SPE Production & Facilities* **20**(1): 5–13. <https://doi.org/10.2118/77497-PA>
- Kumar, R., Dao, E. and Mohanty, K. 2012. Heavy-Oil Recovery by In-Situ Emulsion Formation. *SPE Journal* **17**(02): 326–34. <https://doi.org/10.2118/129914-PA>
- Leaute, R.P. and Carey, B.S. 2007. Liquid Addition to Steam for Enhancing Recovery (LASER) of Bitumen with CSS: Results from the First Pilot Cycle. *Journal of Canadian Petroleum Technology* **46** (9): 22–30. <https://doi.org/10.2118/2005-161>
- Leaute, R.P., 2002. Liquid Addition to Steam for Enhancing Recovery of Bitumen with CSS: Evolution of Technology from Research Concept to a Field Pilot at Cold Lake. Presented at the SPE/Petroleum Society of CIM/CHOA Paper Number 79011, Calgary, Alberta, Canada, November 4-7. <https://doi.org/10.2118/79011-MS>
- Li, W., Mamora, D. D., Li, Y., 2011a. Light-and Heavy-Solvent Impacts on Solvent-Aided-SAGD Process: A Low –Pressure Experimental Study. *Journal of Canadian Petroleum Technology* **50** (4): 19–30. <https://doi.org/10.2118/133277-PA>
- Li, W., Mamora, D. D., Li, Y., 2011b. Solvent-type and –ratio Impacts on Solvent-aided SAGD Process. *SPE Reservoir Evaluation & Engineering* **14** (3): 320–331. <https://doi.org/10.2118/130802-PA>
- Liu, Q., Dong, M., Ma, S. and Tu, Y. 2007. Surfactant enhanced alkaline flooding for Western Canadian heavy oil recovery. *Colloids and Surfaces A: Physicochem. Eng. Aspects* **293**: 63–71. <https://doi.org/10.1016/j.colsurfa.2006.07.013>
- Liu, Q., Dong, M., Yue, X. and Hou, J. 2006. Synergy of alkali and surfactant in emulsification of heavy oil in brine. *Colloids and Surfaces A: Physicochemical and Engineering Aspects* **273**: 219–228. <https://doi.org/10.1016/j.colsurfa.2005.10.016>
- Lu, C., Liu, H., Zhao, W., Lu, K., Liu, Y., Tian, J. and Tan, X. 2017. Experimental Investigation of In-Situ Emulsion Formation To Improve Viscous-Oil Recovery in Steam-Injection Process Assisted by Viscosity Reducer. *SPE Journal* **22**(01): 130–137. <https://doi.org/10.2118/181759-PA>
- Mohammadmoradi, P., Taheri, S., and Kantzas, A. 2017. Interfacial Areas in Athabasca Oil Sands. *Energy & Fuels: An American Chemical Society Journal*, **31**(8): 8131–8145. <https://doi.org/10.1021/acs.energyfuels.7b01458>
- Mohebbati, M. H., Maini, B. B., and Harding, T. G. 2012. Numerical-Simulation Investigation of the Effect of Heavy-oil Viscosity on the Performance of Hydrocarbon Additives in SAGD. *SPE Reservoir Evaluation & Engineering* **15** (02): 165–181. <https://doi.org/10.2118/138151-PA>

- Nasr, T. N., Beaulieu, G., Golbeck, H., Heck, G. 2003. Novel expanding solvent-SAGD process "ES-SAGD". *Journal of Canadian Petroleum Technology* **42** (1): 13–16. <https://doi.org/10.2118/03-01-TN>
- Núñez, V. R. G., Carvalho, M. S., & Basante, V. A. 2009. Oil displacement by oil-water emulsion injection in coreflooding experiments. In *20th International Congress of Mechanical Engineering*.
- Pal, R. 1996. Effect of Droplet Size on the Rheology of Emulsions. *AIChE Journal* **42**(11): 3181–3190. <https://doi.org/10.1002/aic.690421119>
- Pal, R. 2000. Shear Viscosity Behavior of Emulsions of Two Immiscible Liquids. *Journal of Colloid and Interface Science* **225**: 359–366. <https://doi.org/10.1006/jcis.2000.6776>
- Pei, H., Zhang, G., Ge, J., Jin, L. and Ma, C. 2013. Potential of alkaline flooding to enhance heavy oil recovery through water-in-oil emulsification. *Fuel* **104**: 284–293. <https://doi.org/10.1016/j.fuel.2012.08.024>
- Sadowski, T. J., & Bird, R. B. 1965. Non - Newtonian Flow through Porous Media. I. Theoretical. *Transactions of the Society of Rheology*, **9**(2): 243–250. <https://doi.org/10.1122/1.549000>
- Shen, C. 2013. *Enhanced Oil Recovery Field Case Studies*. 1st Edition. Chapter 13, 413 – 455, Elsevier.
- Sheng, K., Okuno, R., and Wang, M. 2018. Dimethyl Ether as an Additive to Steam for Improved Steam-Assisted Gravity Drainage. *SPE Journal*. Accepted for publication on October 17, 2017. <https://doi.org/10.2118/184983-PA>
- Shi, X. and Okuno, R. 2018. Analytical solution for steam-assisted gravity drainage with consideration of temperature variation along the edge of a steam chamber. *Fuel* **217**: 262–274. <https://doi.org/10.1016/j.fuel.2017.12.110>
- Srivastava, P. and Castro, L. 2011. Successful Field Application of Surfactant Additives to Enhance Thermal Recovery of Heavy Oil. SPE Middle East Oil and Gas Show and Conference, 25-28 September, Manama, Bahrain. <https://doi.org/10.2118/140180-MS>
- Tagavifar, M., Herath, S., Weerasooriya, U., Sepehrnoori, K. and Pope, G. 2017. Measurement of Microemulsion Viscosity and Its Implications for the Chemical Enhanced Oil Recovery. *SPE Journal*. <https://doi.org/10.2118/179672-PA>
- Thomas, S., & Farouq Ali, S. M. 1989. Flow of emulsions in porous media, and potential for enhanced oil recovery. *Journal of Petroleum Science & Engineering* **3**(1): 121–136. [https://doi.org/10.1016/0920-4105\(89\)90038-7](https://doi.org/10.1016/0920-4105(89)90038-7)
- Uzoigwe, A., & Marsden, S. S., Jr. 1970. Emulsion Rheology and Flow through Unconsolidated Synthetic Porous Media. In SPE-AIME 45th Annual Fall Meeting, Houston. <https://doi.org/10.2118/3004-MS>
- Venkatramani, A. and Okuno, R. 2015. Characterization of Water-Containing Reservoir Oil Using an EOS for Steam Injection Processes. *Journal of Natural Gas Science and Engineering* **26**: 1091–1106. <http://dx.doi.org/10.1016/j.jngse.2015.07.036>
- Venkatramani, A. and Okuno, R. 2017. Classification of Reservoir Heterogeneity for SAGD and ES-SAGD: Under What Type of Heterogeneity is ES-SAGD More Likely to Lower SOR?. SPE Annual Technical Conference and Exhibition, 9–11 October, 2017, San Antonio, Texas, USA. <https://doi.org/10.2118/187427-MS>
- Xiao, R., Teletzke, G., Lin, M., Glotzbach, R., Aitkulov, A., Yeganeh, M., Jaishankar, A. and Hegner, J. 2017. A Novel Mechanism of Alkaline Flooding to Improve Sweep Efficiency for Viscous Oils. SPE Annual Technical Conference and Exhibition, 9-11 October, San Antonio, Texas, USA. <https://doi.org/10.2118/187366-MS>
- Zeidani, K. and Gupta, S. 2013. Surfactant-Steam Process: An Innovative Enhanced Heavy Oil Recovery Method for Thermal Applications. SPE Heavy Oil Conference-Canada, 11-13 June, Calgary, Alberta, Canada. <https://doi.org/10.2118/165545-MS>